

Correlation functions and coherence lengths in a two-gap superconductor

Artjom Vargunin and Teet Örd*

Institute of Physics, University of Tartu, 4 Tõhe Street, 51010 Tartu, Estonia

(Received 10 July 2012; published 5 September 2012)

We derive analytically the spatial correlation functions for gap fluctuations in a two-band scenario with intraband and interband pair-transfer interactions. These functions demonstrate the changes in functionality due to the presence of two channels of coherency described by the divergent and finite correlation lengths. Even at the phase transition point, both channels are essential for two-band superconductivity. Generally, their relative contributions depend on the temperature and system parameters.

DOI: [10.1103/PhysRevB.86.104506](https://doi.org/10.1103/PhysRevB.86.104506)

PACS number(s): 74.40.Gh, 74.81.-g, 64.60.Ej

I. INTRODUCTION

The theory of superconductivity with overlapping bands has started to develop since 1959;¹ however, only after discovery of multicomponent nature of MgB₂ in 2001 (Ref. 2) and pnictides in 2008 (Ref. 3), the multigap approaches have become an object of exceeding interest.

The peculiarities of the spatial coherency in multiband superconductors have attracted much attention recently in connection with type-1.5 behavior.⁴ In usual one-band systems, there is only one coherence length, the value of which in units of penetration depth determines response to magnetic fields: type-I or type-II. It was suggested that in a two-band superconductor, one has two correlation lengths resulting in much richer physics than type-I/type-II dichotomy. In particular, there is a possibility to observe a mixture of domains of Meissner state and vortex clusters, called type-1.5 superconductivity. The latter regime is supported also by the interband proximity effect⁵ and by different kinds of intercomponent interaction involving Josephson, mixed gradient, or density-density couplings.⁶

The existence of two qualitatively different length scales in a two-band system was demonstrated more than 20 years ago⁷ and recently.^{8,9} Two distinct correlation lengths are also present in the negative- U Hubbard model of two-orbital superconductivity.¹⁰ In this respect, the connection between peculiarities of spatial coherency and excitation of the Leggett mode in two-gap material was discussed.¹¹

Different point of view on the correlation behavior in a two-band model is based on the statement that two order parameters should have identical characteristic lengths of spatial variation by approaching critical temperature.^{12,13} Away from the critical point, two gaps are generally not proportional to each other, and these scales become decoupled.¹⁴ Numeric estimations for the healing lengths of the gaps confirm that conclusion for several superconducting materials.¹⁵ Here, we note that scientific discussion about discrepancy of length scales in the vicinity of critical temperature still continues.¹⁶

Experimentally, the presence of distinct spatial scales in various two-band compounds was evidenced, e.g., by scanning tunneling spectroscopy,¹⁷ muon spin relaxation measurements,¹⁸ and in heat transport features¹⁹ as a function of magnetic field.

In this paper, we analyze inhomogeneous two-band superconductivity in a very natural way by deriving correlation functions for gap fluctuations. The spatial behavior of these char-

acteristics reveals two different correlation lengths describing the joint superconducting condensate as a whole. These length scales are analyzed as the functions of the temperature and interband interaction constant. The competition between the contributions of the corresponding coherency channels to the correlation functions is discussed.

II. DERIVATION OF CORRELATION FUNCTIONS

We start with the two-band superconductivity Hamiltonian

$$H = \sum_{\alpha\mathbf{k}s} \tilde{\epsilon}_{\alpha}(\mathbf{k}) a_{\alpha\mathbf{k}s}^{\dagger} a_{\alpha\mathbf{k}s} - \frac{1}{V} \sum_{\alpha\alpha'} \sum_{\mathbf{k}\mathbf{k}'\mathbf{q}} W_{\alpha\alpha'} a_{\alpha\mathbf{k}\uparrow}^{\dagger} a_{\alpha-\mathbf{k}+\mathbf{q}\downarrow}^{\dagger} a_{\alpha'-\mathbf{k}'+\mathbf{q}\downarrow} a_{\alpha'\mathbf{k}'\uparrow}, \quad (1)$$

where $\tilde{\epsilon}_{\alpha} = \epsilon_{\alpha} - \mu$ is the electron energy in the band, $\alpha = 1, 2$, relative to the chemical potential μ ; V is the volume of superconductor, and $W_{\alpha\alpha'}$ is the matrix element of intraband ($\alpha = \alpha'$) or interband ($\alpha \neq \alpha'$) pair-transfer interaction. It is supposed that the chemical potential is located in the region of the bands overlapping. We assume that (effective) electron-electron interactions are nonzero only in the layer $\mu \pm \hbar\omega_D$ and $W_{\alpha\alpha'}$ is independent on electron wave vector in this layer. For simplicity, we take $W_{12} = W_{21}$.

We calculate the partition function $Z = \text{Sp} \exp(-\frac{H}{k_B T})$ for the macroscopic system by means of Hubbard-Stratonovich transformation.²⁰ For $W^2 = W_{11}W_{22} - W_{12}^2 > 0$ and for real order parameters δ_{α} , the static path approximation reads as

$$Z = \int_{-\infty}^{\infty} e^{-\frac{\tilde{F}}{k_B T}} d\delta_{10} d\delta_{20} \prod_{\mathbf{k} \neq 0}^* d\delta'_{1\mathbf{k}} d\delta'_{1\mathbf{k}} d\delta'_{2\mathbf{k}} d\delta'_{2\mathbf{k}}, \quad (2)$$

$$\tilde{F} = \tilde{F}_n + \sum_{\alpha=1}^2 \int \left(a_{\alpha} \delta_{\alpha}^2 + \frac{b_{\alpha}}{2} \delta_{\alpha}^4 + K_{\alpha} (\nabla \delta_{\alpha})^2 - c \delta_{\alpha} \delta_{3-\alpha} \right) dV. \quad (3)$$

Here, integration variables are treated as real and imaginary parts of Fourier components for nonequilibrium order parameters $\delta_{\alpha}(\mathbf{r}) = \sum_{\mathbf{k}} \delta_{\alpha\mathbf{k}} e^{i\mathbf{k}\mathbf{r}}$, \tilde{F} is nonequilibrium free energy of inhomogeneous system, and $\tilde{F} = \tilde{F}_n$ in the absence of superconductivity. The star sign near multiplication in Z denotes the half of \mathbf{k} space. We do not expand the coefficients

$$a_{\alpha} = \frac{W_{3-\alpha, 3-\alpha}}{W^2} - \rho_{\alpha} \ln \frac{1.13 \hbar \omega_D}{k_B T}, \quad (4)$$

$b_\alpha = \frac{0.11\rho_\alpha}{(k_B T)^2}$, $c = \frac{W_{12}}{W^2}$, and $K_\alpha = \frac{0.02\rho_\alpha \hbar^2 v_{F\alpha}^2}{(k_B T)^2}$ in powers of $T - T_c$, which allows us to apply free energy in the form (3) substantially further from critical temperature T_c . Here ρ_α is the density of states at the Fermi level, and $v_{F\alpha}$ is the Fermi velocity in the corresponding band. Note that the coefficient K_α used alludes to isotropic situation.

The homogeneous equilibrium state is defined by the minimization $\frac{\delta \tilde{F}}{\delta \Delta_\alpha} |_{\Delta_\alpha = \Delta_\alpha} = 0$, which gives us the set of equations for coupled homogeneous order parameters $\Delta_{1,2}$, namely,

$$a_\alpha \Delta_\alpha + b_\alpha \Delta_\alpha^3 = c \Delta_{3-\alpha}. \quad (5)$$

One should also take into account the relation between phases in equilibrium $\text{sqn}(c \Delta_1 \Delta_2) = +1$. The critical point is determined by condition $a_1(T_c) a_2(T_c) = c^2$, which has two solutions $T_{c\pm}$ and $T_{c-} > T_{c+}$. If $T_{c\alpha}$ are intrinsic transition temperatures in the bands and $T_{c1} > T_{c2}$, then for $W_{12} \rightarrow 0$ we have $T_{c-} \rightarrow T_{c1}$ and $T_{c+} \rightarrow T_{c2}$. Note that in the system with coupled bands, there is only one phase transition point $T_c = T_{c-}$.

Now, we linearize functional \tilde{F} near homogeneous state with free energy F_h by assuming $\delta_\alpha(\mathbf{r}) = \Delta_\alpha + \eta_\alpha(\mathbf{r})$. By means of complex Fourier components $\eta_{\alpha\mathbf{k}}$ we have

$$\tilde{F} = F_h + V \sum_{\alpha=1}^2 \left(A_{\alpha 0} \eta_{\alpha 0}^2 - c \eta_{\alpha 0} \eta_{3-\alpha 0} + 2 \sum_{\mathbf{k} \neq 0}^* [A_{\alpha\mathbf{k}} (\eta_{\alpha\mathbf{k}}^2 + \eta_{\alpha\mathbf{k}}'^2) - c (\eta_{\alpha\mathbf{k}}' \eta_{3-\alpha\mathbf{k}}' + \eta_{\alpha\mathbf{k}}'' \eta_{3-\alpha\mathbf{k}}'')] \right), \quad (6)$$

where $A_{\alpha\mathbf{k}} = A_\alpha + K_\alpha \mathbf{k}^2$ and $A_\alpha = a_\alpha + 3b_\alpha \Delta_\alpha^2 \geq 0$. Note that due to interband pairing, there appear nondiagonal terms in the quadratic form (6). Statistics for the equilibrium state fluctuations is determined by the distribution function $e^{-\frac{\tilde{F}}{k_B T}}$ normalized to Z . By using Gaussian approximation (6), we calculate mean values $\langle \eta_{\alpha\mathbf{k}} \eta_{\alpha'\mathbf{k}}^* \rangle$ and then correlation functions $\Gamma_{\alpha\alpha'}(\mathbf{r} - \mathbf{r}') = \sum_{\mathbf{k}} \langle \eta_{\alpha\mathbf{k}} \eta_{\alpha'\mathbf{k}}^* \rangle e^{i\mathbf{k}(\mathbf{r}-\mathbf{r}')}$ for the order-parameter fluctuations considered at different points separated by distance $|\mathbf{r} - \mathbf{r}'| \neq 0$. We obtain $\Gamma_{\alpha\alpha'} = \Gamma_{\alpha\alpha'}^+ + \Gamma_{\alpha\alpha'}^-$, where

$$\Gamma_{\alpha\alpha'}^\pm = \mp \frac{k_B T}{8\pi K_\alpha} \frac{\xi_\mp^2 (\xi_\pm^2 - \xi_{3-\alpha}^2) \exp\left(-\frac{|\mathbf{r}-\mathbf{r}'|}{\xi_\pm}\right)}{\xi_{3-\alpha}^2 (\xi_\pm^2 - \xi_\mp^2) |\mathbf{r} - \mathbf{r}'|} \quad (7)$$

and

$$\Gamma_{12}^\pm = \mp \frac{k_B T}{8\pi K_1 K_2} \frac{\xi_\pm^2 \xi_\mp^2 c \exp\left(-\frac{|\mathbf{r}-\mathbf{r}'|}{\xi_\pm}\right)}{\xi_\mp^2 - \xi_\pm^2} \frac{1}{|\mathbf{r} - \mathbf{r}'|}. \quad (8)$$

Note also that $\Gamma_{12} = \Gamma_{21}$. In Eqs. (7) and (8), we have introduced $\xi_\alpha^2 = \frac{K_\alpha}{A_\alpha}$ and the correlation lengths ξ_\pm are given by

$$\xi_\pm^2 = \frac{2\xi_1^2 \xi_2^2}{\xi_1^2 + \xi_2^2 \pm \sqrt{(\xi_1^2 - \xi_2^2)^2 + 4\xi_1^2 \xi_2^2 \frac{c^2}{A_1 A_2}}}. \quad (9)$$

These quantities have the following properties. For finite interband pairing, $\xi_- > \xi_+ > 0$. In the temperature region where $\xi_1 > \xi_2$, one has $\xi_- > \xi_1$ and $\xi_+ < \xi_2$. For the opposite case $\xi_1 < \xi_2$, we get $\xi_- > \xi_2$ and $\xi_+ < \xi_1$. As a result, $\Gamma_{\alpha\alpha'}^\pm > 0$. However, depending on the sign of interband interaction constant, one contribution in Γ_{12} becomes negative.

The characteristics ξ_\pm define the size of the region, where the order-parameter fluctuations are significantly correlated. In fact, these length scales appear in the exponents despite the band index taken for the correlation functions, i.e., ξ_\pm describe joint superconducting state rather than individual bands. We note also that ξ_\pm coincide with the correlation lengths⁹ found by means of inhomogeneous gap equations.

III. RESULTS AND DISCUSSIONS

A. Correlation lengths

The presence of interacting order parameters makes the coherence properties of the two-band system quite different from the corresponding characteristics in single-band superconductors. To analyze the physics of the one-band case, one should take $c \rightarrow 0$. In this limit, $\xi_\pm \rightarrow \xi_\alpha|_{c=0}$, i.e., one obtains two separate correlation lengths attributed to the band $\alpha = 1, 2$. Each length diverges at its own point given by intrinsic transition temperature $T_{c\alpha}$. Note that $\xi_- \rightarrow \xi_1|_{c=0}$ and $\xi_+ \rightarrow \xi_2|_{c=0}$ in the temperature region where $\xi_1|_{c=0} > \xi_2|_{c=0}$, however, $\xi_- \rightarrow \xi_2|_{c=0}$ and $\xi_+ \rightarrow \xi_1|_{c=0}$ for the temperatures where $\xi_1|_{c=0} < \xi_2|_{c=0}$. Further, we assume for specificity $T_{c2} < T_{c1}$, i.e., the condition $\xi_1|_{c=0} < \xi_2|_{c=0}$ corresponds to the lower-temperature region, while $\xi_1|_{c=0} > \xi_2|_{c=0}$ to the higher temperatures in the superconducting state.

Nonzero coupling between bands modifies drastically the trivial physics of two noninteracting condensates. The coherency is described by lengths ξ_\pm which become tricky combinations of band characteristics ξ_α [see Eq. (9)]. To illustrate the evolution of ξ_\pm with model parameters we fix intra-band ones: $W_{11,22} = 0.3$ eV cell, $\rho_{1,2} = (1, 0.94)$ (eV cell)⁻¹, $v_{F1,2} = (5, 5.104) \times 10^5$ m/s, cell = 0.1 nm³. For these values $T_{c2} = 0.81 T_{c1}$. We also assume parabolic electron spectrum where $\frac{\rho_2}{\rho_1} = \left(\frac{v_{F1}}{v_{F2}}\right)^3$.

Figure 1 shows temperature dependencies for correlation lengths together with the evolution of homogeneous gaps calculated numerically as interband coupling increases. We see that ξ_- and ξ_+ as functions of the temperature are remarkably different. First, the length ξ_- behaves critically diverging at phase transition point T_c . At the same time, ξ_+ remains finite. Second, ξ_- can change below T_c very nonmonotonically, while the temperature dependence of ξ_+ is substantially weaker.^{8,9} The appearance of additional maximum in superconducting phase for ξ_- is strongly supported by the smaller values of W_{12} , representing the memory effect about criticality in the band $\alpha = 2$. The position of this maximum is correlated with the inflection point of the smaller gap, which takes place in the vicinity of T_{c2} . As was pointed out earlier,²¹ the nonmonotonicity of the critical coherence length elucidates the temperature behavior of the gaps' healing length²² and vortex size²³ in a superconductor with weakly interacting bands.

One can argue that the scheme based on the expansion (3) is applicable only close to the critical point. We note that the coefficients (4) taken allow us to go essentially further below T_c . For the comparison, we have plotted in Fig. 1 homogeneous gaps calculated numerically by means of microscopic theory. The latter are approximated by the solutions of system (5) very well in the temperature region considered.

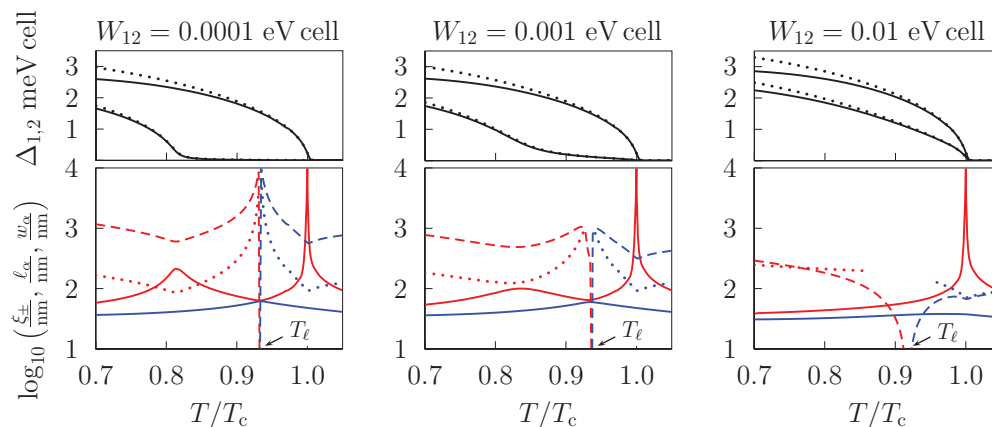


FIG. 1. (Color online) Above: The plots of the gaps Δ_α as a solution of Eqs. (5) (solid lines) and derived microscopically (dotted lines) vs temperature for various interband couplings W_{12} . Below: The log plots of ξ_- (solid red lines), ξ_+ (solid blue lines), ℓ_1 (dashed red lines), ℓ_2 (dashed blue lines), w_1 (70%) (dotted red lines), and w_2 (70%) (dotted blue lines) vs temperature for same W_{12} . The parameters ℓ_α and w_α characterize the efficiency of critical and noncritical channels in the structure of correlation functions (see main text), and T_ℓ is the temperature where ℓ_α goes to zero.

Due to the definition of the critical point $a_1(T_c)a_2(T_c) = c^2$ and the relation $A_\alpha(T_c) = a_\alpha(T_c)$, one obtains

$$\xi_+^2(T_c) = \frac{\xi_1^2(T_c)\xi_2^2(T_c)}{\xi_1^2(T_c) + \xi_2^2(T_c)}, \quad (10)$$

and zero for the denominator of $\xi_-(T_c)$, i.e., the latter length diverges precisely at T_c . This implies that only length scale ξ_- can be attributed directly to the superconducting phase transition in a two-band model. In the vicinity of T_c , we get

$$\xi_-^2 = \begin{cases} c^2 \frac{\xi_1^2(T_c) + \xi_2^2(T_c)}{\rho_1 a_2(T_c) + \rho_2 a_1(T_c)} \frac{T_c}{T - T_c}, & T > T_c \\ c^2 \frac{\xi_1^2(T_c) + \xi_2^2(T_c)}{2 \rho_1 a_2(T_c) + \rho_2 a_1(T_c)} \frac{T_c}{T_c - T}, & T < T_c. \end{cases} \quad (11)$$

Both expressions (10) and (11) one meets in the literature.⁷ Note also that in the approach¹² claiming the existence of two divergent correlation lengths, the latter coincide with ξ_- in the vicinity of the critical point.

Next, we denote the factor in Eq. (11) by $\xi_-^2(0)$, the value of the formula (11) at $T = 0$, and analyze $\xi_-(0)$ and $\xi_+(T_c)$ as the functions of interband interaction. Figure 2 shows

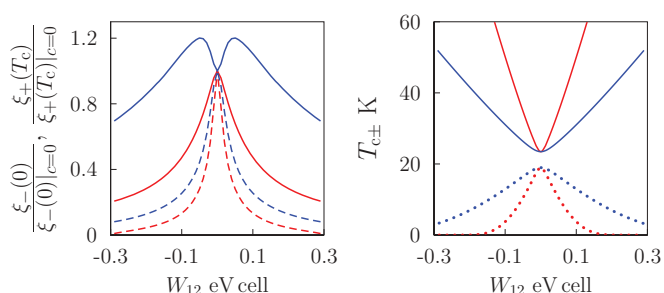


FIG. 2. (Color online) Left: The plots of $\xi_-(0)$ (solid lines) and $\xi_+(T_c)$ (dashed lines) normalized to their values at $W_{12} = 0$ vs interband coupling W_{12} . Right: The plots of $T_c = T_{c-}$ (solid lines) and T_{c+} (dotted lines) vs W_{12} . Red curves correspond to the parameters given in text, blue ones to the modified parameters in band $\alpha = 2$, namely, $W_{22} = 2.26$ eV cell, $\rho_2 = 0.13$ (eV cell)⁻¹, $v_{F2} = 10^6$ m/s. For these values, we have the same ratio $T_{c2} = 0.81T_{c1}$.

these dependencies for different sets of intraband parameters. Analytic consideration indicates that $\xi_+(T_c)$ always decreases with $|W_{12}|$, while $\xi_-(0)$ can pass through a maximum at some finite value of W_{12} . We interpret this feature as follows. The one-band limit $c = 0$ gives $T_c = T_{c1}$ and $a_1(T_{c1}) = 0$. As a result, $\xi_-^2|_{c=0} = \frac{K_1(T_{c1})}{2\rho_1} \frac{T_{c1}}{T_{c1} - T}$ for $T < T_{c1}$. This is a standard one-band expression for the squared correlation length expanded near the critical point. The factor $\xi_-^2(0)|_{c=0} = \frac{K_1(T_{c1})}{2\rho_1}$ is proportional to $\frac{1}{T_{c1}^2}$, i.e., $\xi_-(0)|_{c=0}$ decreases with the critical temperature increase and vice versa. In the two-band system, T_c always grows with W_{12} (see Fig. 2) and one can expect the reduction of $\xi_-(0)$ with an increase of $|W_{12}|$ by analogy with the single-band case. However, in the two-component situation, especially for weak interband couplings, the memory effect related to the lower intrinsic phase transition is strong. The latter is characterized by the temperature T_{c+} , which always decreases with $|W_{12}|$ (see Fig. 2). By analogy with the one-band case, it can lead to the rise of $\xi_-(0)$. Thus, there are two opposite tendencies associated with the temperatures $T_{c\pm}$ which govern the behavior of $\xi_-(0)$ as a function of interband coupling. By analyzing this competition analytically, we find that if

$$\frac{v_{F2}}{v_{F1}} < \sqrt{1 + 2 \frac{\rho_1 W_{11} - \rho_2 W_{22}}{(\rho_1 W_{11})^2}}, \quad (12)$$

$\xi_-(0)$ has a maximum, whereas for the opposite sign in Eq. (12) the function $\xi_-(0)$ has a minimum at $W_{12} = 0$. We believe that nonmonotonicity of $\xi_-(0)$ is a clear footprint of the two-band nature near the critical point.

One comment should be made about noncritical coherence length. The quantity ξ_+^2 is always finite and decreases as the strength of interband interaction increases, crossing zero at $W^2 = 0$. At the same time, there is a natural lower bound for coherence lengths in the Ginzburg-Landau theory defined by the microscopic length scales $\frac{\hbar v_{F\alpha}}{k_B T_c \pi}$ (Cooper-pair size in the bands). The latter guarantees the smallness of the gradient term in the Ginzburg-Landau expansion. To estimate the maximal

value of ξ_+ , we use Eq. (10) for $c = 0$. We find

$$\xi_+(T_c)|_{c=0} = \xi_2(T_{c1})|_{c=0} \sim \frac{1}{\sqrt{\rho_1 W_{11} - \rho_2 W_{22}}}. \quad (13)$$

Consequently, the value of $\xi_+(T_c)$ can be magnified when T_{c2} approaches T_{c1} . In this process, noncritical coherence length can surpass microscopic lengths,⁹ i.e., two length scales of coherency found are meaningful even in the standard two-band Ginzburg-Landau model for relevant parameters. To overcome the restriction related to the microscopic lengths, one should take into account the higher terms of the gradient expansion in the Ginzburg-Landau approach. In this way, one gets better agreement with microscopic theory.²¹ However, the theory based on two-band Eilenberger equations also predicts the disappearance of noncritical length for strong interband pairings at $W^2 \approx 0$.⁸ The absence of the real noncritical correlation length may signal spatial periodicity of fluctuations of two-gap superconductivity.¹¹

B. Correlation functions

Interaction between bands results in more complicated structure of correlation functions as compared to the case of decoupled bands for which

$$\Gamma_{\alpha\alpha} = \frac{k_B T}{8\pi K_\alpha |\mathbf{r} - \mathbf{r}'|} e^{-\frac{|\mathbf{r}-\mathbf{r}'|}{\xi_\alpha|_{c=0}}}, \quad \Gamma_{12} = 0. \quad (14)$$

Next, we discuss the correlation functions for nonvanishing interband pairings.

First, we consider different spatial regions. For shorter distances $|\mathbf{r} - \mathbf{r}'| \ll \xi_+ < \xi_-$ (denote as “sd”), we obtain from Eqs. (7) and (8)

$$\Gamma_{\alpha\alpha}^{\text{sd}} \approx \frac{k_B T}{8\pi K_\alpha |\mathbf{r} - \mathbf{r}'|}, \quad \Gamma_{12}^{\text{sd}} \approx \frac{k_B T c}{8\pi K_1 K_2} \frac{\xi_+ \xi_-}{\xi_+ + \xi_-}. \quad (15)$$

In this fully correlated case, the functions $\Gamma_{\alpha\alpha'}$ are maximal. If $\xi_1(T_c) \gg \xi_2(T_c)$, then near T_c the main contribution to Γ_{11}^{sd} stems from the critical, and to Γ_{22}^{sd} from the noncritical, channel of coherency and vice versa. Note that condition $\xi_1(T_c) \gg \xi_2(T_c)$ is supported by the smaller interband interaction.

For larger distances $\xi_+ < \xi_- \ll |\mathbf{r} - \mathbf{r}'|$ (denote as “ld”), the functions $\Gamma_{\alpha\alpha'}^{\text{ld}}$ are defined mostly by critical contributions and they vanish. By approaching T_c , we have in this regime $\xi_+ \ll |\mathbf{r} - \mathbf{r}'| \ll \xi_-$ and

$$\Gamma_{\alpha\alpha}^{\text{ld}} \approx \frac{k_B T_c}{8\pi K_\alpha(T_c) |\mathbf{r} - \mathbf{r}'|}, \quad K_\alpha = K_\alpha \frac{\xi_1^2 + \xi_2^2}{\xi_\alpha^2}, \quad (16)$$

$$\Gamma_{12}^{\text{ld}} \approx \frac{k_B T_c c}{8\pi K_1(T_c) K_2(T_c)} \frac{\xi_+^2(T_c)}{|\mathbf{r} - \mathbf{r}'|}. \quad (17)$$

Thus, at the critical point, Γ_{12} changes in space from constant value Γ_{12}^{sd} to the function Γ_{12}^{ld} which decreases linearly with logarithm of $\frac{|\mathbf{r}-\mathbf{r}'|}{\xi_+}$. The disagreement between K_α and K_α characterizes the behavior of $\Gamma_{\alpha\alpha}$. If $\xi_1(T_c) \gg \xi_2(T_c)$, then Γ_{11}^{sd} and Γ_{11}^{ld} are the very same function at T_c , but there is remarkable difference in the dependencies Γ_{22}^{sd} and Γ_{22}^{ld} related to the change of the dominant coherency channel from the noncritical to the critical one. This transformation is also noticeable in Fig. 3, and it is supported by the weaker interband couplings. For the opposite situation $\xi_1(T_c) \ll \xi_2(T_c)$, we have

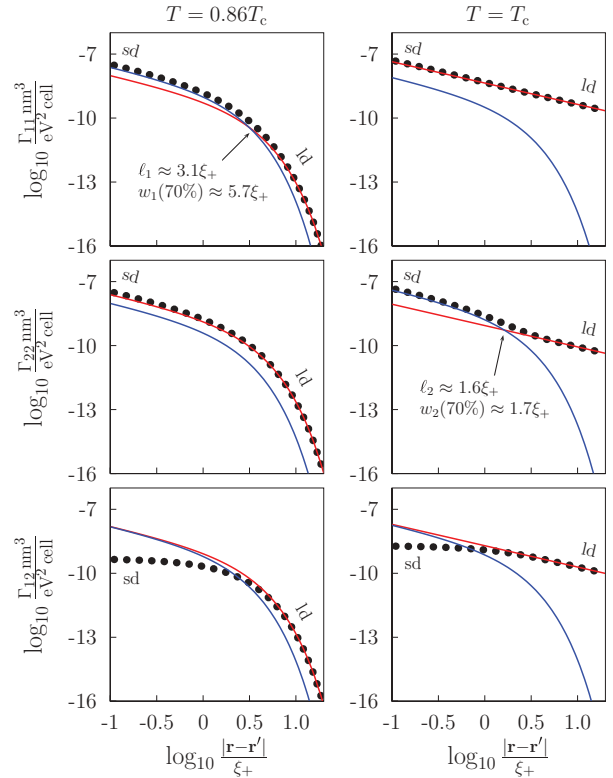


FIG. 3. (Color online) The log plots of $\Gamma_{\alpha\alpha'}$ (dots) together with corresponding contributions $\Gamma_{\alpha\alpha'}^+$ (red line), $\Gamma_{\alpha\alpha'}^-$ and $|\Gamma_{12}^+|$ (blue line) vs distance $|\mathbf{r} - \mathbf{r}'|$ for $T = 0.86T_c$ (left column) and $T = T_c$ (right column). Here, $W_{12} = 0.01$ eV cell and intraband parameters as in text. At T_c , we have $\frac{\xi_1}{\xi_2} \approx 2.2$. The regimes “sd” and “ld” are discussed in the text.

different dependencies for Γ_{11}^{sd} and Γ_{11}^{ld} , but the same for Γ_{22}^{sd} and Γ_{22}^{ld} . Therefore, the changes in spatial functionality of the correlation functions are intrinsic for two-gap superconductors.

To estimate the efficiency of different correlation channels, we find the distance ℓ_α where $\Gamma_{\alpha\alpha}^+ = \Gamma_{\alpha\alpha}^-$,

$$\ell_1 = \frac{\xi_+ \xi_-}{\xi_- - \xi_+} \ln \frac{1 - \frac{\xi_2^2}{\xi_+^2}}{\frac{\xi_2^2}{\xi_-^2} - 1} = -\ell_2. \quad (18)$$

One obtains $\ell_1 > 0$ in the region where $\xi_1(T) < \xi_2(T)$ and vice versa. Whereas the driving role in the behavior of $\Gamma_{\alpha\alpha}$ passes from the noncritical channel to the critical one at the distance ℓ_α , that interchange takes place at fixed temperature only for certain correlation function, Γ_{11} or Γ_{22} . Figure 1 shows that ℓ_α can substantially exceed ξ_- , especially for nearly decoupled bands. In this case, the value $\Gamma_{\alpha\alpha}(\ell_\alpha)$ is vanishing, i.e., the noncritical channel dominates for all reasonable distances. At T_c , one finds $\ell_2 = \xi_+ \ln \frac{\xi_1^2}{\xi_2^2}$.

Intraband correlation functions are characterized by different types of coexistence of the contributions from two coherency channels involved: total domination of one (critical) channel or interchange of driving role between them. The border between these regimes is defined by the temperature T_ℓ , the point where $\xi_1 = \xi_2$ or, alternatively, $\ell_\alpha = 0$. The position of T_ℓ is sensitive to the model parameters. If $v_{F1} > v_{F2}$, one

has $T_\ell < T_c$. However, for $v_{F1} < v_{F2}$, there is a value

$$|W_{12}| = \frac{v_{F1}v_{F2}}{v_{F2}^2 - v_{F1}^2} \frac{\rho_1 W_{11} - \rho_2 W_{22}}{\sqrt{\rho_1 \rho_2}}, \quad (19)$$

for which $T_\ell = T_c$, and for stronger interband interaction $T_\ell > T_c$.

Finally, the relative contribution $\frac{\Gamma_{\alpha\alpha}^+}{\Gamma_{\alpha\alpha}^-}$ decreases and $\frac{\Gamma_{\alpha\alpha}^-}{\Gamma_{\alpha\alpha}^+}$ increases with distance. If $\ell_\alpha \geq 0$, these functions cross at ℓ_α , i.e., $\frac{\Gamma_{\alpha\alpha}^+}{\Gamma_{\alpha\alpha}^-} \geq \frac{\Gamma_{\alpha\alpha}^-}{\Gamma_{\alpha\alpha}^+}$ for tiny $|\mathbf{r} - \mathbf{r}'|$. We define the width w_α of interchange region as the size of the spatial area around ℓ_α where $\frac{\Gamma_{\alpha\alpha}^+}{\Gamma_{\alpha\alpha}^-}$ and $\frac{\Gamma_{\alpha\alpha}^-}{\Gamma_{\alpha\alpha}^+}$ simultaneously do not exceed fixed percentage $p > 50\%$. We find

$$w_\alpha(p) = \frac{\xi_+ \xi_-}{\xi_- - \xi_+} \ln \frac{p^2}{(1-p)^2}. \quad (20)$$

At T_c , one obtains $w_\alpha \sim \xi_+$, i.e., different channels interchange on the distance defined by the noncritical length scale. The width w_α shrinks at T_c with an increase of interband coupling. For nearly decoupled bands, $w_1 \sim \xi_+$ holds also in the vicinity of T_{c2} , however, w_1 grows with W_{12} at those temperatures (see Fig. 1). Note that the noncritical channel can significantly dominate only away from the region around T_ℓ where $\frac{\Gamma_{\alpha\alpha}^+}{\Gamma_{\alpha\alpha}^-} < p$ even for tiny $|\mathbf{r} - \mathbf{r}'|$. The latter region widens with interband

interaction increase, and it is seen as the temperature gap between the curves $w_{1,2}$ in Fig. 1.

IV. CONCLUSIONS

The spatial evolution of correlation functions for two-band superconductivity indicates the presence of two distinct channels of coherency described by the critical (divergent at critical point) and noncritical (finite at critical point) correlation lengths. Although these characteristics are not related directly to the bands, two-component nature manifests itself in the nonmonotonicities of critical length scale as a function of the temperature and the strength of interband interaction. The features of the competition between coherency channels involved depend on the temperature as well as model parameters. This picture should be taken into account in the interpretation of the experiments and in the creation of relevant theories, e.g., type-1.5 superconductivity.

ACKNOWLEDGMENT

This study was supported by the European Union through the European Regional Development Fund (Centre of Excellence ‘‘Mesosystems: Theory and Applications,’’ TK114) and by the Estonian Science Foundation (Grant No. 8991).

*teet.ord@ut.ee

¹H. Suhl, B. T. Matthias, and L. P. Walker, *Phys. Rev. Lett.* **3**, 552 (1959); V. A. Moskalenko, *Fiz. Met. Met.* **8**, 503 (1959).

²S. Tsuda, T. Yokoya, T. Kiss, Y. Takano, K. Togano, H. Kito, H. Ihara, and S. Shin, *Phys. Rev. Lett.* **87**, 177006 (2001); A. A. Zhukov, L. F. Cohen, K. Yates, G. K. Perkins, Y. Bugoslavsky, M. Polichetti, A. Berenov, J. L. Macmanus Driscoll, A. D. Caplin, L. Hao, and J. Gallop, *Supercond. Sci. Technol.* **14**, L13 (2001); Y. Wang, T. Plackowski, and A. Junod, *Phys. C (Amsterdam)* **355**, 179 (2001); F. Bouquet, R. A. Fisher, N. E. Phillips, D. G. Hinks, and J. D. Jorgensen, *Phys. Rev. Lett.* **87**, 047001 (2001).

³K. Matano, Z. A. Ren, X. L. Dong, L. L. Sun, Z. X. Zhao, and G. Q. Zheng, *Europhys. Lett.* **83**, 57001 (2008); Y. L. Wang, L. Shan, L. Fang, P. Cheng, C. Ren, and H. H. Wen, *Supercond. Sci. Technol.* **22**, 015018 (2009); F. Hunte, J. Jaroszynski, A. Gurevich, D. C. Larbalestier, R. Jin, A. S. Sefat, M. A. McGuire, B. C. Sales, D. K. Christen, and D. Mandrus, *Nature (London)* **453**, 903 (2008).

⁴E. Babaev and M. Speight, *Phys. Rev. B* **72**, 180502(R) (2005); V. Moshchalkov, M. Menghini, T. Nishio, Q. H. Chen, A. V. Silhanek, V. H. Dao, L. F. Chibotaru, N. D. Zhigadlo, and J. Karpinski, *Phys. Rev. Lett.* **102**, 117001 (2009).

⁵E. Babaev, J. Carlström, and M. Speight, *Phys. Rev. Lett.* **105**, 067003 (2010); E. Babaev and J. Carlström, *Phys. C (Amsterdam)* **470**, 717 (2010).

⁶J. Carlström, E. Babaev, and M. Speight, *Phys. Rev. B* **83**, 174509 (2011).

⁷Y. M. Poluektov and V. V. Krasilnikov, *Fiz. Nizk. Temp.* **15**, 1251 (1989).

⁸M. Silaev and E. Babaev, *Phys. Rev. B* **84**, 094515 (2011).

⁹T. Örd, K. Rågo, and A. Vargunin, *J. Supercond. Novel Magn.* **25**, 1351 (2012).

¹⁰G. Litak, T. Örd, K. Rågo, and A. Vargunin, *Acta Phys. Pol. A* **121**, 747 (2012); *Phys. C (Amsterdam)* (to be published).

¹¹N. Kristofel, T. Örd, and P. Rubin, *Supercond. Sci. Technol.* **22**, 014006 (2009).

¹²V. G. Kogan and J. Schmalian, *Phys. Rev. B* **83**, 054515 (2011).

¹³J. Geyer, R. M. Fernandes, V. G. Kogan, and J. Schmalian, *Phys. Rev. B* **82**, 104521 (2010).

¹⁴A. A. Shanenko, M. V. Milošević, F. M. Peeters, and A. V. Vagov, *Phys. Rev. Lett.* **106**, 047005 (2011).

¹⁵L. Komendová, M. V. Milošević, A. A. Shanenko, and F. M. Peeters, *Phys. Rev. B* **84**, 064522 (2011).

¹⁶E. Babaev and M. Silaev, *Phys. Rev. B* **86**, 016501 (2012); V. G. Kogan and J. Schmalian, *ibid.* **86**, 016502 (2012).

¹⁷M. R. Eskildsen, M. Kugler, S. Tanaka, J. Jun, S. M. Kazakov, J. Karpinski, and O. Fischer, *Phys. Rev. Lett.* **89**, 187003 (2002).

¹⁸S. Serventi, G. Allodi, R. DeRenzi, G. Guidi, L. Romanò, P. Manfrinetti, A. Palenzona, C. Niedermayer, A. Amato, and C. Baines, *Phys. Rev. Lett.* **93**, 217003 (2004).

¹⁹E. Boaknin, M. A. Tanatar, J. Paglione, D. G. Hawthorn, R. W. Hill, F. Ronning, M. Sutherland, L. Taillefer, J. Sonier, S. M. Hayden, and J. W. Brill, *Phys. C (Amsterdam)* **408–410**, 727 (2004).

²⁰J. Hubbard, *Phys. Rev. Lett.* **3**, 77 (1959); R. L. Stratonovich, *Dokl. Fiz. Nauk.* **114**, 1097 (1958) [*Sov. Phys. Dokl.* **2**, 416 (1958)].

²¹M. Silaev and E. Babaev, *Phys. Rev. B* **85**, 134514 (2012).

²²L. Komendová, Y. Chen, A. A. Shanenko, M. V. Milošević, and F. M. Peeters, *Phys. Rev. Lett.* **108**, 207002 (2012).

²³R. Geurts, M. V. Milošević, and F. M. Peeters, *Phys. Rev. B* **81**, 214514 (2010).